

FORMALDEHYDE IN COMETS C/1995 O1 (HALE-BOPP), C/2002 T7 (LINEAR), AND C/2001 Q4 (NEAT): INVESTIGATING THE COMETARY ORIGIN OF H₂CO

STEFANIE N. MILAM,¹ ANTHONY J. REMIJAN,^{2,3,4,5} MARIA WOMACK,⁶ LEIF ABRELL,⁷ L. M. ZIURYS,¹ SUSAN WYCKOFF,⁸
A. J. APPONI,¹ D. N. FRIEDEL,² L. E. SNYDER,² J. M. VEAL,^{2,9} PATRICK PALMER,¹⁰ L. M. WOODNEY,¹¹
MICHAEL F. A'HEARN,¹² J. R. FORSTER,¹³ M. C. H. WRIGHT,¹³
I. DE PATER,¹³ S. CHOI,⁶ AND M. GESMUNDO⁶

Received 2006 March 16; accepted 2006 June 2

ABSTRACT

Observations of formaldehyde (H₂CO) have been conducted toward comets C/1995 O1 (Hale-Bopp), C/2001 Q4 (NEAT), and C/2002 T7 (LINEAR) using the Arizona Radio Observatory (ARO) 12 m telescope at 1.2 and 2 mm. Aperture synthesis maps of H₂CO at 3 mm were made using the Berkeley-Illinois-Maryland Association (BIMA) interferometer toward comet Hale-Bopp. These data indicate that the production rate of H₂CO is $\sim 3.7 \times 10^{28} \text{ s}^{-1}$ at ~ 1 AU in comet Hale-Bopp, using a simple Monte Carlo model, if a nuclear origin for the molecule is assumed. However, maps of H₂CO in Hale-Bopp, in comparison with CO, show an extended distribution ($r_s \sim 15,000$ km) with small-scale structure oriented roughly along the comet-Sun direction. This result suggests a source of H₂CO other than the comet nucleus. The extended source of formaldehyde is probably grains composed of a mixture of silicates and organic material. The production rate for H₂CO increases to $Q \sim 1.4 \times 10^{29} \text{ s}^{-1}$ assuming such an extended grain source. This value implies a $Q/Q(\text{H}_2\text{O}) \sim 1.4\%$, which is similar to the production rate ratio of $Q/Q(\text{H}_2\text{O}) \sim 4\%$ derived from in situ measurements of H₂CO in comet Halley. Production rates for H₂CO toward comets C/2002 T7 (LINEAR) and C/2001 Q4 (NEAT) are 1.4×10^{27} and $5.6 \times 10^{26} \text{ s}^{-1}$, respectively, modeled using the extended grain source. The spectra of H₂CO measured toward comet C/2002 T7 (LINEAR) show evidence for a second velocity component, most likely arising from comet fragmentation.

Subject headings: astrobiology — comets: individual (Hale-Bopp (C/1995 O1), NEAT (C/2001 Q4), LINEAR (C/2002 T7)) — radio lines: solar system — techniques: interferometric

1. INTRODUCTION

The close approach of comet C/1995 O1 (Hale-Bopp) provided an observational flourish of molecular lines, including detections of over 10 new cometary species. These molecules ranged from simple diatomics to complex organic compounds, for example, sulfur monoxide (SO), hydrogen sulfide (H₂S), formic acid (HCOOH), formamide (NH₂CHO), and ethylene

glycol (HOCH₂CH₂OH; see Bockelée-Morvan et al. 2000; Woodney et al. 1996; Crovisier et al. 2004; Lis et al. 1999). These successes were partly due to the fact that comet Hale-Bopp was visible for a record 569 days and reached a peak visual magnitude of -1 .

In the spring of 2004, two long-period comets crossed the sky with peak visual magnitudes of ~ 2 : comets C/2001 Q4 (NEAT) and C/2002 T7 (LINEAR). Comet C/2001 Q4 (NEAT) was originally discovered in August of 2001. However, H₂O was not detected in this comet until 2004 March 6.6 (UT) by Lecacheux et al. (2004). The measured production rate of $Q(\text{H}_2\text{O}) \sim 1.3 \times 10^{29} \text{ s}^{-1}$ at a heliocentric distance of $R_h \sim 1.5$ AU was found to be similar to that of comet Halley (Mumma et al. 1986). Comet C/2002 T7 (LINEAR) was first discovered in 2002 mid-October and reached perihelion on 2004 April 23. This comet was a dynamically new Oort cloud object, as evidenced by its slightly hyperbolic orbit at perihelion. From 2004 April 10 to 17, Howell et al. (2004) observed the 18 cm OH lines, which are good tracers of H₂O production. Their average measured OH production rate was $Q(\text{OH}) \sim 2.5 \times 10^{29} \text{ s}^{-1}$ ($R_h \sim 0.6$ AU), again similar to that of comet Halley at perihelion. In both comets, a variety of other molecules were observed as well, predominantly in 2004 May. Species such as hydrogen cyanide (HCN), hydrogen isocyanide (HNC), carbon monosulfide (CS), formaldehyde (H₂CO), methanol (CH₃OH), and carbon monoxide (CO) were detected in both objects, by single-dish and aperture synthesis techniques (Küppers et al. 2004; Friedel et al. 2005; Remijan et al. 2006; Magee-Sauer et al. 2004).

As these observations, as well as others, have demonstrated, a vast number of cometary molecules found are organic, including CH₃OH, H₂CO, NH₂CHO, and HOCH₂CH₂OH. Both CH₃OH

¹ NASA Astrobiology Institute, Department of Chemistry, Department of Astronomy, and Steward Observatory, 933 North Cherry Avenue, University of Arizona, Tucson, AZ 85721; stemil@as.arizona.edu, lziurys@as.arizona.edu, aapponi@as.arizona.edu.

² Department of Astronomy, University of Illinois, 1002 West Green Street, Urbana, IL 61801; friedel@astro.uiuc.edu, snyder@astro.uiuc.edu.

³ NASA Goddard Space Flight Center, Computational and Information Sciences and Technologies Office, Code 606, Greenbelt, MD 20771.

⁴ National Research Council Resident Research Associate.

⁵ Current address: National Radio Astronomy Observatory, 520 Edgemont Road, Charlottesville, VA 22903; aremijan@nrao.edu.

⁶ Department of Physics and Astronomy, St. Cloud State University, St. Cloud, MN 56301; mwomack@stcloudstate.edu.

⁷ Department of Chemistry, NASA Astrobiology Institute, University of Arizona, 1306 East University Boulevard, Tucson, AZ 85721; abrell@u.arizona.edu.

⁸ Department of Physics and Astronomy, Arizona State University, Tempe, AZ 85287.

⁹ Current address: Southwestern College, 900 Otay Lakes Road, Chula Vista, CA 91910; jveal@swc.cc.ca.us.

¹⁰ Department of Astronomy and Astrophysics, University of Chicago, Chicago, IL 60637; ppalmer@oskar.uchicago.edu.

¹¹ Department of Physics, California State University, San Bernardino, CA 92407; woodney@csusb.edu.

¹² Department of Astronomy, University of Maryland, College Park, MD 20742-2421; ma@astro.umd.edu.

¹³ Department of Astronomy, University of California, Berkeley, CA 94720; rforster@astro.berkeley.edu, wright@astro.berkeley.edu, imke@floris.berkeley.edu.

TABLE 1
OBSERVATIONS AND ABUNDANCES OF H₂CO AND CO TOWARD HALE-BOPP, Q4 NEAT, AND T7 LINEAR

Comet	Line	Telescope	Transition	UT Date	ν (MHz)	θ_b (arcsec)	D (km)	η_c	T_R^* (K)	$\Delta v_{1/2}$ (km s ⁻¹)	R_h (AU)	Δ (AU)
Hale-Bopp.....	H ₂ CO	12 m	2 _{1,2} → 1 _{1,1}	1997 Mar 11.99	140839.5	45	44648	0.78	0.18 ± 0.03	2.0 ± 0.9	1.0	1.4
		12 m	2 _{0,2} → 1 _{0,1}	1996 May 31.45	145603.0	43	107315	0.76	0.04 ± 0.02	0.8 ± 0.5	4.2	3.4
		12 m	2 _{1,1} → 1 _{1,0}	1996 May 28.28	150498.3	42	106799	0.75	0.02 ± 0.01	4.4 ± 2.0	4.3	3.5
	CO	12 m ^a	3 _{1,2} → 2 _{1,1}	1997 Mar 28.60	225697.8	28	27009	0.53	0.75 ± 0.34	2.0 ± 0.6	0.9	1.3
		BIMA	1 _{0,1} → 0 _{0,0}	1997 Mar 24.83	72838.0	...	10499	...	1.10 ± 0.32 ^c	1.0 ± 0.5	0.9	1.3
		12 m ^a	2 → 1	1997 Apr 7.61	230538.0	27	27611	0.5	0.66 ± 0.33	1.7 ± 0.3	0.9	1.4
Q4 NEAT.....	H ₂ CO	BIMA	1 → 0	1997 Apr 7.93	115271.2	...	8181	...	2.35 ± 0.49 ^c	1.8 ± 0.5	0.9	1.4
		12 m	3 _{1,3} → 2 _{1,2}	2004 May 26.19	211211.4	30	14883	0.57	0.04 ± 0.02	0.9 ± 0.7	1.0	0.7
T7 LINEAR.....	H ₂ CO	12 m	3 _{0,3} → 2 _{0,2}	2004 May 15.03	218222.2	29	8729	0.55	0.02 ± 0.01	1.4 ± 0.7	1.0	0.4
		12 m	3 _{1,3} → 2 _{1,2}	2004 May 25.01	211211.4	30	7724	0.57	0.04 ± 0.02	1.6 ± 0.7	0.9	0.4
		12 m	3 _{0,3} → 2 _{0,2}	2004 May 15.60	218222.2	29	6794	0.55	0.09 ± 0.02	2.1 ± 0.7	0.8	0.3
		12 m	3 _{1,2} → 2 _{1,1}	2004 May 15.73	225697.8	28	6559	0.53	0.08 ± 0.02	2.0 ± 0.7	0.8	0.3

^a OTF map data.

^b Synthesized beam for BIMA observations of H₂CO (11''2 × 10''4) and CO (8''8 × 6''1).

^c Intensity given in Jy beam⁻¹, which corresponds to 2.2 K for H₂CO and 4.02 K for CO in these observations.

and H₂CO are considered to be interstellar precursors to the diose, glycolaldehyde (CH₂OHCHO; e.g., Halfen et al. 2006; Sorrell 2001). Terrestrially, CH₂OHCHO is a precursor to the aldopentose ribose, which is a key component to ribonucleic acid (RNA). In the interstellar medium, CH₂OHCHO has been detected in the extended regions surrounding the high-mass star-forming region Sgr B2(N) (Hollis et al. 2001, 2004; Halfen et al. 2006). The detection of this complex species may indicate that some part of the synthesis of large prebiotic organic molecules originated in the interstellar medium. Furthermore, the detection of these large compounds in comets may support planetary “seeding” through the disruption of cometary bodies at they approach perihelion, thus ejecting prebiotic material into planetary atmospheres.

As part of an ongoing investigation to establish the contribution of molecular clouds to prebiotic synthesis, we have been conducting observations of simple organic molecules in cometary gases. Because of its importance in the formation of ribose via the formose reaction, measurements have focused on H₂CO. This molecule is also of interest because it is speculated that it may originate from a polymer, polyoxymethylene [(CH₂O)_n, n = 2, 3, 4, ...] in comets. Here we report detections of the $J = 1 \rightarrow 0$, $J = 2 \rightarrow 1$, and $J = 3 \rightarrow 2$ transitions of H₂CO and the $J = 1 \rightarrow 0$ and $J = 2 \rightarrow 1$ lines of CO toward comet C/1995 O1 (Hale-Bopp), using the former National Radio Astronomy Observatory (NRAO) Kitt Peak 12 m telescope, now run by the Arizona Radio Observatory (ARO), and the Berkeley-Illinois-Maryland Association (BIMA) interferometer. In addition, the $J = 3 \rightarrow 2$ transitions of H₂CO were observed toward comets C/2002 T7 (LINEAR) and C/2001 Q4 (NEAT) with the ARO 12 m telescope. From these data, column densities and production rates have been determined for H₂CO and CO for each comet. Using the BIMA observations, a comparison of the distributions for these molecules around the nucleus of Hale-Bopp has also been made. Here we present our analysis and discuss the origin of H₂CO in cometary material.

2. OBSERVATIONS

2.1. Arizona Radio Observatory 12 m

Observations of H₂CO and CO toward comet C/1995 O1 (Hale-Bopp) (hereafter, comet Hale-Bopp) were taken during two observing runs in 1996 May and 1997 March using the former

NRAO 12 m telescope on Kitt Peak, AZ.¹⁴ Observations of H₂CO toward comets C/2002 T7 (LINEAR) (hereafter, comet T7 LINEAR) and C/2001 Q4 (NEAT) (hereafter, comet Q4 NEAT) were conducted from 2004 May to June, also using the 12 m telescope, now run by ARO. Dual-channel SIS mixers were used for the 2 and 1.2 mm bands, operated in single-sideband mode with ~20 dB image rejection. Back ends used for these observations were individual filter banks with 100, 250, or 500 kHz resolutions, as well as the millimeter autocorrelator (MAC) with resolutions of 791 or 98 kHz. The spectral temperature scale was determined by the chopper-wheel method, corrected for forward spillover losses, given in terms of T_R^* (in K). The radiation temperature, T_R , is then derived from the corrected beam efficiency, η_c , where $T_R = T_R^*/\eta_c$. A two-body ephemeris program was used to determine the comet’s position using the orbital elements provided by D. Yeomans (1996 and 2004, private communication) of JPL (Jet Propulsion Laboratory). Focus and positional accuracy were checked periodically on nearby planets or masers. Data were taken in position-switched mode with the off position 30' west in azimuth.

On-the-fly maps of H₂CO and CO toward comet Hale-Bopp were also conducted at the ARO 12 m telescope from 1997 mid-March to early April. The 250 kHz resolution filter bank was principally employed for these measurements. The images have the following sample spacings, or angular separation of the dish beam size projected onto the sky per sample output, in R.A. and decl.: CO, (10''7, 7''9); and H₂CO, (10''6, 7''9). Observing frequencies, dates, beam size (θ_b), diameter of the projected beam size on the comet (D), and comet distances at the times of measurements are listed in Table 1.

2.2. BIMA Array

Comet Hale-Bopp was observed using the “soft” C configuration of the BIMA array¹⁵ from 1997 March to April. Data were acquired in interferometric (cross-correlation) mode with nine antennas. The minimum baseline for these observations was ~15 m,

¹⁴ The National Radio Astronomy Observatory is a facility of the National Science Foundation operated under cooperative agreement by the Associated Universities, Inc. The Kitt Peak 12 m telescope is currently operated by the Arizona Radio Observatory (ARO), Steward Observatory, University of Arizona, with partial funding from the Research Corporation.

¹⁵ Operated by the University of California, Berkeley, the University of Illinois, and the University of Maryland with support from the National Science Foundation.

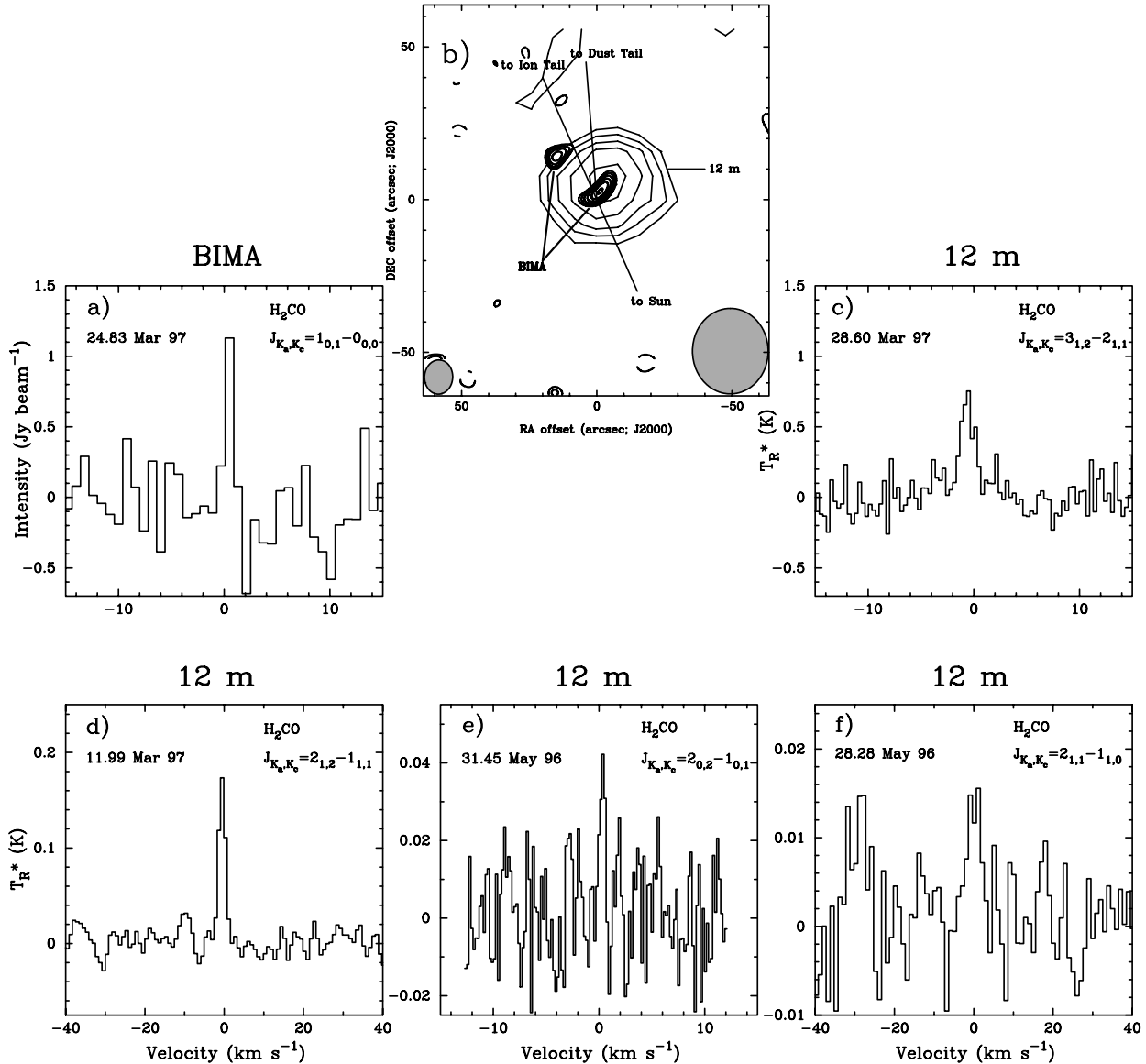


FIG. 1.—Comet C/1995 O1 (Hale-Bopp) single-field H₂CO images and spectra taken with the BIMA array and ARO 12 m radio telescope. The observation date is located at the top left corner of each spectrum. (a) H₂CO $J_{K_a, K_c} = 1_{0,1} \rightarrow 0_{0,0}$ cross-correlation spectrum of the distribution in (b) at 72.838 GHz taken with the BIMA array; the ordinate is flux density per beam (Jy beam^{-1} , $1 \sigma \sim 0.3 \text{ Jy beam}^{-1}$). (b) Hale-Bopp emission contours (*bold*) from the BIMA array of the $J_{K_a, K_c} = 1_{0,1} \rightarrow 0_{0,0}$ transition of H₂CO and emission contours (*normal*) from the ARO 12 m of the $J_{K_a, K_c} = 3_{1,2} \rightarrow 2_{1,1}$ transition. The bold contour levels are $-0.825, 0.750, 0.825, 0.900, 0.975, 1.050,$ and $1.125 \text{ Jy beam}^{-1}$. The normal contour levels are 0.9, 1.2, 1.5, 1.8, and 2.1 K, for $\int T_R dV$. Image coordinates (in arcseconds) are offsets relative to the predicted position of the nucleus. The synthesized beam ($11''.22 \times 10''.41$) of the BIMA array is in the lower left. The beam size ($28''$) of the ARO 12 m is in the lower right. The line segments show the directions to the ion and dust tails and toward the Sun. (c) H₂CO $J_{K_a, K_c} = 3_{1,2} \rightarrow 2_{1,1}$ center spectrum of the distribution in (b) at 225.698 GHz taken at the ARO 12 m with 250 kHz resolution; the ordinate is the chopper wheel antenna temperature, T_R^* (K, $1 \sigma \sim 0.3 \text{ K}$). (d) H₂CO $J_{K_a, K_c} = 2_{1,2} \rightarrow 1_{1,1}$ spectrum at 140.840 GHz taken at the ARO 12 m with 391 kHz resolution at $\sim 1 \text{ AU}$ ($1 \sigma \sim 0.03 \text{ K}$). (e) H₂CO $J_{K_a, K_c} = 2_{0,2} \rightarrow 1_{0,1}$ spectrum at 145.603 GHz taken at the ARO 12 m with 100 kHz resolution at $\sim 4 \text{ AU}$ ($1 \sigma \sim 0.02 \text{ K}$). (f) H₂CO $J_{K_a, K_c} = 2_{1,1} \rightarrow 1_{1,0}$ spectrum at 150.498 GHz taken at the ARO 12 m with 500 kHz resolution at $\sim 4 \text{ AU}$ ($1 \sigma \sim 0.01 \text{ K}$). All spectra are plotted in a cometocentric velocity frame.

and the maximum baseline was $\sim 139 \text{ m}$. The synthesized beamwidths in R.A. and decl. for CO and H₂CO are ($8''.8, 6''.1$) and ($11''.2, 10''.4$), respectively. Typical system temperatures ranged from $\sim 200 \text{ K}$ at high elevations to $\sim 400 \text{ K}$ at low elevations. The spectral windows containing these transitions had a bandwidth of 25 MHz and were divided into 256 channels for a spectral resolution of $0.1 \text{ MHz channel}^{-1}$. However, to increase the signal-to-noise ratio in each window, the data were averaged over two channels, giving an effective spectral resolution of $0.2 \text{ MHz channel}^{-1}$, which corresponds to $\sim 0.52 \text{ km s}^{-1}$ for CO and $\sim 0.80 \text{ km s}^{-1}$ for H₂CO.

Table 1 also lists the parameters for the BIMA array observations. The source used to calibrate the antenna-based gains was

0102+584 for both H₂CO and CO observations, with a 0.30 and $0.40 \text{ Jy beam}^{-1}$ channel rms, respectively. Intensities of H₂CO and CO were 2.2 and 4.2 Jy beam^{-1} , which are equivalent to 2.20 and 4.02 K in these observations. The absolute amplitude calibration of these sources was based on planetary observations and is accurate to within $\sim 20\%$. All data were corrected to JPL ephemeris reference orbit 139. The data were combined and imaged using the MIRIAD software package (Sault et al. 1995).

3. RESULTS

Formaldehyde is a slightly asymmetric top species with C_{2v} symmetry with an a -dipole moment of $\mu_a = 2.3 \text{ D}$ (Shoolery & Sharbaugh 1951). Consequently, transitions in H₂CO follow

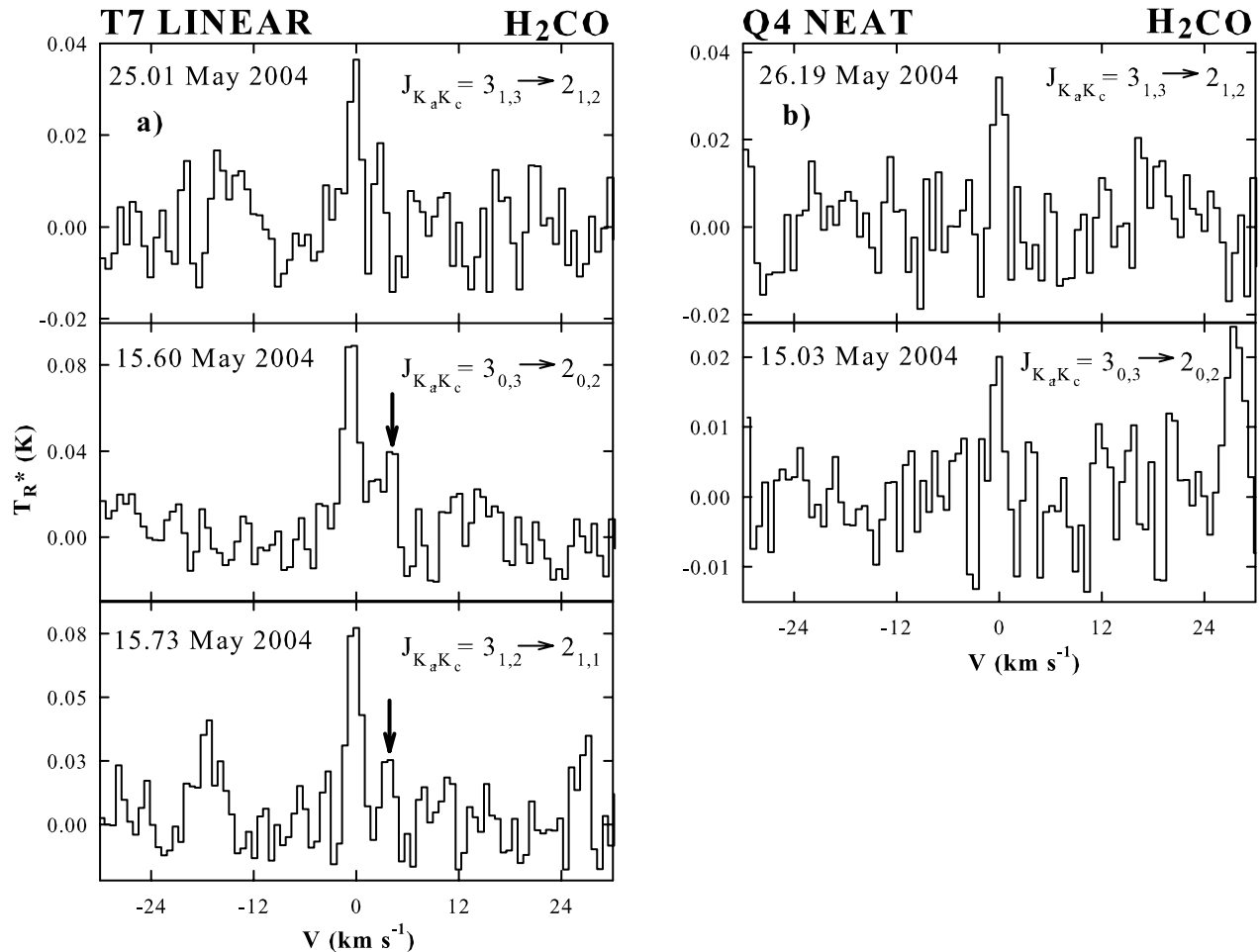


FIG. 2.—(a) Comet C/2002 T7 (LINEAR) observations of $\text{H}_2\text{CO } J_{K_a, K_c} = 3_{1,3} \rightarrow 2_{1,2}$, $3_{0,3} \rightarrow 2_{0,2}$, and $3_{1,2} \rightarrow 2_{1,1}$ transitions from the ARO 12 m telescope in 2004 May. A second velocity component is present in the 2004 May 15 data at approximately 4 km s^{-1} . (b) Comet C/2001 Q4 (NEAT) observations of $\text{H}_2\text{CO } J_{K_a, K_c} = 3_{1,3} \rightarrow 2_{1,2}$ and $3_{0,3} \rightarrow 2_{0,2}$ transitions from the ARO 12 m telescope in 2004 May. All spectra are plotted in a cometocentric velocity frame with 500 kHz resolution.

α -dipole selection rules of $\Delta J = 0, \pm 1$; $\Delta K_a = 0$; and $\Delta K_c = \pm 1$. Therefore, the $J = 1 \rightarrow 0$, $J = 2 \rightarrow 1$, and $J = 3 \rightarrow 2$ transitions each consist of several asymmetry components. Most of these components were observed for each transition.

Figure 1 displays the maps and spectra of H_2CO observed toward comet Hale-Bopp, plotted in a cometocentric velocity frame. The UT date of each observed transition is located in the top left corner of the plotted spectrum. Figure 1d shows the $J_{K_a, K_c} = 2_{1,2} \rightarrow 1_{1,1}$ transition of H_2CO detected toward comet Hale-Bopp at the 12 m, as it approached perihelion. It is quite strong compared to the other two $J = 2 \rightarrow 1$ transitions (Figs. 1e and 1f) observed in 1996 May, almost a year before perihelion. This difference likely arises from the variation in heliocentric distance of the comet during the respective observations (see Table 1). However, these spectra definitively establish the presence of H_2CO toward comet Hale-Bopp, as all three asymmetry components of the $J = 2 \rightarrow 1$ transition were detected.

Figure 1b shows the map of the $J_{K_a, K_c} = 1_{0,1} \rightarrow 0_{0,0}$ line of H_2CO toward comet Hale-Bopp, made with the BIMA array (*bold contours*), overlaid with the on-the-fly (OTF) map of the $J_{K_a, K_c} = 3_{1,2} \rightarrow 2_{1,1}$ transition from the 12 m (*normal contours*). The spectra for the distributions in Figure 1b, measured by BIMA and the 12 m, are plotted with a cometocentric velocity frame in Figures 1a and 1c, respectively. The $J = 3 \rightarrow 2$ emission from the 12 m indicates a somewhat extended source (cf. beam sizes on

map), while the $J = 1 \rightarrow 0$ emission is centered on two distinct clumps. One clump is virtually outside the contour of the $J = 3 \rightarrow 2$ emission. These differences probably arise from the variation in beam sizes, measurement techniques (single dish vs. interferometer), and excitation conditions of the two lines. (The $J = 3 \rightarrow 2$ transition traces higher densities than the $J = 1 \rightarrow 0$ line.) In addition, the formaldehyde emission shows slight horizontal asymmetry around the cometary nucleus in the 12 m map; this is more apparent in the map derived on 1997 April 6.6, which had twice the integration time (see Womack et al. 2000). In the BIMA map, made with $\sim 10''$ resolution, the nuclear component is asymmetric with an elongation similar to that of the 12 m. The separated second component lies tailward of the nucleus.

Figure 2 displays the H_2CO detections toward comets Q4 NEAT and T7 LINEAR from the ARO 12 m telescope. The $J = 3 \rightarrow 2$ transition toward comet T7 LINEAR was observed in all three asymmetry components (Fig. 2a), while only two components were measured toward comet Q4 NEAT due to time constraints and weather (Fig. 2b). Detection of multiple transitions confirms the presence of H_2CO in these comets. In addition, the comet T7 LINEAR data also appear to exhibit a possible second velocity component $\sim 4 \text{ km s}^{-1}$ redward of the main line in the $J_{K_a, K_c} = 3_{0,3} \rightarrow 2_{0,2}$ transition on 2004 May 16. The $J_{K_a, K_c} = 3_{1,2} \rightarrow 2_{1,1}$ transition, although it has a lower signal-to-noise ratio, supports the presence of the second component observed the

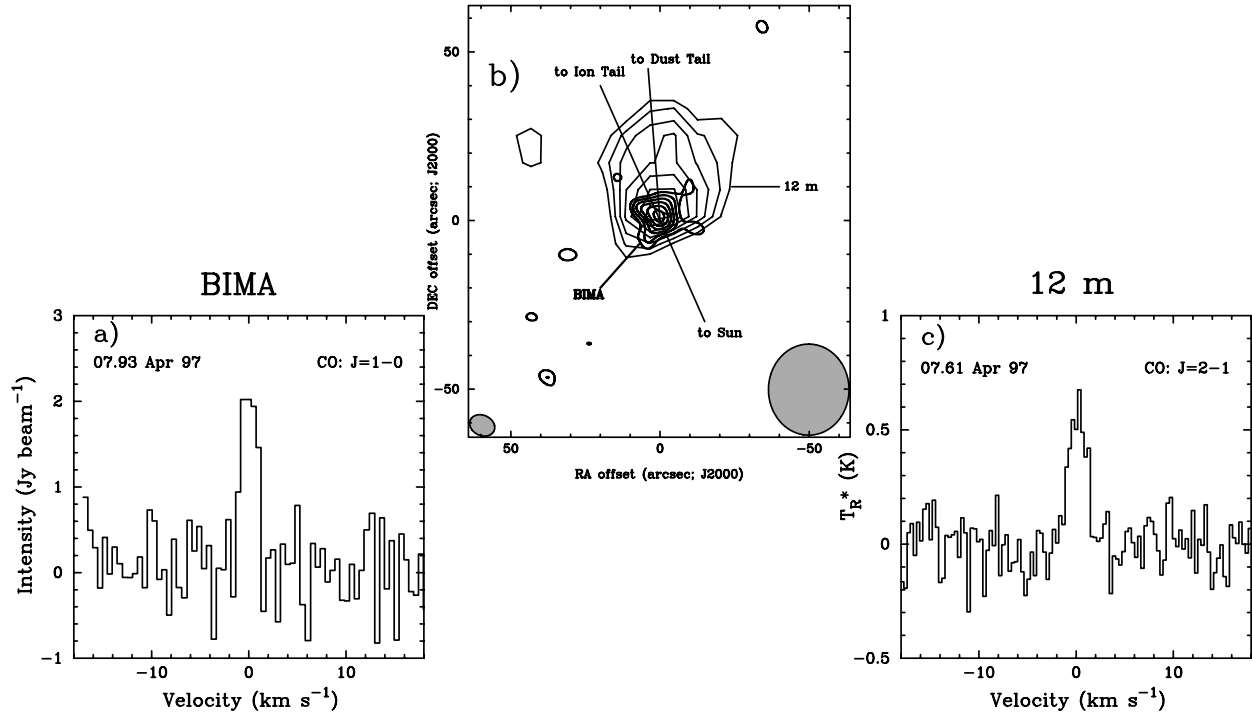


FIG. 3.—Comet C/1995 O1 (Hale-Bopp) single-field CO images and spectra taken with the BIMA array and ARO 12 m radio telescope. The observation date is located at the top left corner of each spectrum. (a) CO $J = 1 \rightarrow 0$ cross-correlation spectrum of distribution in (b) at 115.271 GHz taken with the BIMA array; the ordinate is flux density per beam (Jy beam^{-1} , $1 \sigma \sim 0.5 \text{ Jy beam}^{-1}$). (b) Hale-Bopp emission contours (*bold*) from the BIMA array of the $J = 1 \rightarrow 0$ transition of CO and emission contours (*normal*) from the ARO 12 m of the $J = 2 \rightarrow 1$ transition. The bold contour levels are $-0.8, 0.6, 0.8, 1.0, 1.2, 1.4$, and 1.6 Jy beam^{-1} . The normal contour levels are $1.05, 1.20, 1.35, 1.50, 1.65, 1.80$, and 1.95 K , for $\int T_R dV$. Image coordinates (in arcseconds) are offsets relative to the predicted position of the nucleus. The synthesized beam ($8''.6 \times 6''.1$) of the BIMA array is in the lower left. The beam size ($27''$) of the ARO 12 m is in the lower right. The line segments show the directions to the ion and dust tails and toward the Sun. (c) CO $J = 2 \rightarrow 1$ center spectrum from distribution in (b) at 230.538 GHz taken at the ARO 12 m with 250 kHz resolution; the ordinate is the chopper wheel antenna temperature, T_R^* (K, $1 \sigma \sim 0.2 \text{ K}$). Both spectra are plotted in a cometocentric velocity frame.

same day. This result is similar to that found for comet Hale-Bopp, where a second velocity component was also observed in HCO⁺ and HNC with a velocity shift of 7 km s^{-1} relative to the main feature (Milam et al. 2004).

For comparison, observations of CO toward comet Hale-Bopp were conducted with both facilities. Figure 3 shows the maps and spectra of the $J = 1 \rightarrow 0$ and $J = 2 \rightarrow 1$ transitions of CO toward comet Hale-Bopp. In Figure 3b, the BIMA data of the $J = 1 \rightarrow 0$ transition near 115 GHz (*bold contours*) are overlaid on the 12 m OTF map of the $J = 2 \rightarrow 1$ transition near 230 GHz (*normal contours*). Figures 3a and 3c show the spectra for each map with a cometocentric velocity frame. The emission is more extended than the projected beam sizes for each facility, and a tailward “wing” is present in the 12 m data. The 12 m OTF map of CO shows elongation toward the dust tail, possibly associated CO emission with dust particles. This extension was not observed in the BIMA data. It was most likely resolved out due to the higher spatial resolution of the interferometer.

4. DISCUSSION

4.1. Column Densities, Production Rates, and Abundances

Abundances were derived for H₂CO and CO assuming that the source filled the beams of both telescopes. The formalism for calculating column densities using BIMA array data can be found in Friedel et al. (2005). The column density for 12 m observations was calculated from

$$N_{\text{tot}} = (3kT_R \Delta v_{1/2} \zeta_{\text{rot}}) / (8\pi^3 \nu S_{ij} \mu_0^2 e^{-\Delta E/kT_{\text{rot}}}), \quad (1)$$

where ν is the frequency, T_R is the line temperature corrected for efficiency, $\Delta v_{1/2}$ is the FWHM line width, S_{ij} is the line strength, μ_0 is the permanent dipole moment, ζ_{rot} is the rotational partition function, and N_{tot} is the total number of molecules observed in the beam. The rotational temperature, T_{rot} , was assumed to be 50 K for $R_h \sim 1 \text{ AU}$ and 15 K for $R_h \sim 4 \text{ AU}$, based on the values derived for CH₃OH from Biver et al. (1997). This value is somewhat lower than that determined from Biver et al. (2002), because H₂CO has a larger dipole moment than CH₃OH. Hence, its rotational temperature should be lower. This rotational temperature may not apply to CO, which, in contrast, has a smaller dipole moment relative to CH₃OH; however, for consistency in the calculations it was assumed. Line widths for all three comets were typically $1\text{--}2 \text{ km s}^{-1}$, within the quoted errors.

The column densities derived for CO and H₂CO are listed in Table 2. There is some scatter among these values, because they were measured on different dates and with varying beam sizes. The values for H₂CO are slightly higher in comet Hale-Bopp ($N_{\text{tot}} \sim 7.4 \times 10^{13} \text{ cm}^{-2}$, $\sim 1 \text{ AU}$) compared to comets T7 LINEAR ($N_{\text{tot}} \sim 2 \times 10^{12} \text{ cm}^{-2}$) and Q4 NEAT ($N_{\text{tot}} \sim 5 \times 10^{11} \text{ cm}^{-2}$). This result is expected because of the higher water production rate of comet Hale-Bopp. The CO column densities for comet Hale-Bopp are 2.1×10^{16} and $1.4 \times 10^{15} \text{ cm}^{-2}$ for the $J = 1 \rightarrow 0$ and $J = 2 \rightarrow 1$ transitions, respectively. The difference in column density values, which vary by a factor of 15, is expected because the brightness distribution is centrally peaked and different beam sizes were used.

Table 2 also summarizes the production rates of the molecules observed toward the three comets. The photodissociation rates from Huebner et al. (1992), as well as the abundance ratio with

TABLE 2
COLUMN DENSITIES, PHOTODESTRUCTION RATES, AND PRODUCTION RATES FOR H₂CO AND CO

COMET	LINE	TELESCOPE	TRANSITION	R_h (AU)	N_{tot} (cm ⁻²)	ν_{pd} (s ⁻¹)	Q (s ⁻¹)		$Q/Q(\text{H}_2\text{O})$ (%)	
							Parent	Grain	Parent	Grain
Hale-Bopp	H ₂ CO	12 m	2 _{1,2} → 1 _{1,1}	1.0	5.9 ± 2.8 × 10 ¹²	2.8 × 10 ⁻⁴	2.66 × 10 ²⁸	9.06 × 10 ²⁸	0.3 ^a	0.9 ^a
			2 _{0,2} → 1 _{0,1}	4.2	1.8 ± 1.4 × 10 ¹¹	...	2.68 × 10 ²⁶	1.24 × 10 ²⁷	0.3 ^b	1.2 ^b
			2 _{1,1} → 1 _{1,0}	4.3	4.8 ± 3.2 × 10 ¹¹	...	6.94 × 10 ²⁶	3.06 × 10 ²⁷	0.7 ^b	3.1 ^b
		12 m (OTF) BIMA	3 _{1,2} → 2 _{1,1}	0.9	1.5 ± 0.8 × 10 ¹³	...	2.82 × 10 ²⁸	9.67 × 10 ²⁸	0.3 ^a	1.0 ^a
			1 _{0,1} → 0 _{0,0}	0.9	2.0 ± 1.2 × 10 ¹⁴	...	5.64 × 10 ²⁸	2.19 × 10 ²⁹	0.6 ^a	2.2 ^a
			CO 12 m (OTF) BIMA	2 → 1	0.9	1.4 ± 0.7 × 10 ¹⁵	1.2 × 10 ⁻⁶	3.25 × 10 ²⁹	2.54 × 10 ²⁹	3.2 ^a
1 → 0	0.9	2.1 ± 0.7 × 10 ¹⁶		...	2.09 × 10 ³⁰	1.50 × 10 ³⁰	20.9 ^a	15.0 ^a		
Q4 NEAT	H ₂ CO	12 m	3 _{1,3} → 2 _{1,2}	1.0	3.5 ± 3.0 × 10 ¹¹	2.8 × 10 ⁻⁴	1.79 × 10 ²⁶	6.51 × 10 ²⁶	0.1 ^c	0.5 ^c
			3 _{0,3} → 2 _{0,2}	1.0	5.8 ± 4.1 × 10 ¹¹	...	1.09 × 10 ²⁶	4.61 × 10 ²⁶	0.1 ^c	0.4 ^c
T7 LINEAR	H ₂ CO	12 m	3 _{1,3} → 2 _{1,2}	0.9	6.2 ± 4.1 × 10 ¹¹	2.8 × 10 ⁻⁴	1.03 × 10 ²⁶	4.36 × 10 ²⁶	0.1 ^d	0.2 ^d
			3 _{0,3} → 2 _{0,2}	0.8	3.9 ± 1.6 × 10 ¹²	...	6.63 × 10 ²⁶	2.69 × 10 ²⁷	0.2 ^d	0.8 ^d
			3 _{1,2} → 2 _{1,1}	0.8	1.6 ± 0.7 × 10 ¹²	...	2.52 × 10 ²⁶	1.04 × 10 ²⁷	0.1 ^d	0.3 ^d

^a $Q(\text{H}_2\text{O}) \sim 1 \times 10^{31} \text{ s}^{-1}$ at $R_h \sim 1$ AU from Harris et al. (2002).

^b $Q(\text{H}_2\text{O}) \sim 1 \times 10^{29} \text{ s}^{-1}$ at $R_h \sim 4$ AU from Biver et al. (1997).

^c $Q(\text{H}_2\text{O}) \sim 1.3 \times 10^{29} \text{ s}^{-1}$ at $R_h \sim 1.5$ AU from Lecacheux et al. (2004).

^d $Q(\text{OH}) \sim 3.2 \times 10^{29} \text{ s}^{-1}$ at $R_h \sim 0.6$ AU from Howell et al. (2004).

respect to water (in percent), are listed in this table. Assuming H₂CO and CO are parent species, production rates were determined from a Monte Carlo model. The Monte Carlo model traces the trajectories of molecules, within the telescope beam, ejected from the comet surface. The observed column density is then matched for an output molecular production rate, Q . The CO production rate for comet Hale-Bopp in this case was $\sim 1 \times 10^{30} \text{ s}^{-1}$ (1 AU), based on both observed transitions, implying $Q/Q(\text{H}_2\text{O}) \sim 12\%$. These values are reasonably consistent with those measured by Bockelée-Morvan et al. (2000), who found $Q/Q(\text{H}_2\text{O}) \sim 23\%$. The average H₂CO production rate for comet Hale-Bopp, derived from the Monte Carlo model, was $\sim 3.7 \times 10^{28} \text{ s}^{-1}$ with a $Q/Q(\text{H}_2\text{O})$ of 0.4% at ~ 1 AU. In comparison, Bockelée-Morvan et al. (2000) predict a $Q/Q(\text{H}_2\text{O})$ for H₂CO of 1.1% with their Haser model assuming a nuclear source.

The Hale-Bopp production rate for H₂CO was also calculated using a modified Monte Carlo model, based on the work by Combi & Fink (1997). Here it is assumed that all the H₂CO is released from small ($\sim 0.2 \mu\text{m}$) organic refractory particles (such as CHON grains), which are expanding with a constant velocity from the nucleus. A single grain radius and velocity are assumed to represent the average of an ensemble of particles constituting the expanding grain halo. Such grains decouple collisionally from the inner coma gas ~ 300 km from the nucleus at a terminal velocity $v_g \sim 0.5 \text{ km s}^{-1}$ at 1 AU (Gombosi & Horanyi 1986). The grains then become superheated to temperatures ~ 500 K (Lamy & Perrin 1988; Combi & Fink 1997; Kolokolova et al. 2004), releasing gaseous H₂CO from the grains directly into the coma, with no intermediate dissociation or thermal degradation assumed. Each H₂CO molecule is then released from a grain in a random direction with a constant velocity $v_d = v_0 R_h^{-1/4}$, where $v_0 = 0.6 \text{ km s}^{-1}$ (Combi & Fink 1997). The radial extent of the distributed grain halo inferred from the observed H₂CO spatial distribution at 1 AU is $R_{\text{gh}} \sim 10^4 \text{ km}$ (see Fig. 1). Thus, the estimated CHON-like grain lifetime is $\tau_g = R_{\text{gh}}/v_g \sim 2 \times 10^4 \text{ s}$.

Following Combi & Fink (1997), it was assumed that the size of each grain decreases linearly with time (since the grain evaporation rate and the surface area are both assumed to scale with the square of the grain radius). Each H₂CO molecule is released from a grain after some time interval, t_i , given by the probability distribution, $P = (1 - t_i/\tau_g)^2$ (Combi & Fink 1997). Using

Monte Carlo precepts, this release time can be expressed as $t_i = \tau_g [1 - (1 - R_i)^{1/2}]$, where R_i is a random number in the interval 0–1. Each H₂CO molecule subsequently photodissociates in the solar UV radiation field on the usual randomized exponential timescale, $t_d = -\tau_d \ln(1 - R_i)$ (Combi & Fink 1997; Combi & Smyth 1988), where τ_d is the H₂CO photodissociation timescale, scaled to the appropriate heliocentric distance (Huebner et al. 1992).

This grain model yields an average production rate for H₂CO toward comet Hale-Bopp at ~ 1 AU of $Q(\text{H}_2\text{CO}) \sim 1.4 \times 10^{29} \text{ s}^{-1}$ (see Table 2) with $Q/Q(\text{H}_2\text{O}) \sim 1.4\%$. An increase of about a factor of 4 is therefore found. This model was also used for determining the CO production rate, which was found to be $Q(\text{CO}) \sim 8.8 \times 10^{29} \text{ s}^{-1}$ with $Q/Q(\text{H}_2\text{O}) \sim 9\%$. The grain model results do not increase the production rate from the nuclear model for CO ($Q \sim 1 \times 10^{30} \text{ s}^{-1}$), indicating that the CO lifetime is too long for a significant variation between models. The large difference in the H₂CO and CO production rates derived here for comet Hale-Bopp confirms that H₂CO cannot be an important source of CO in the comet.

4.2. Spatial Distribution of H₂CO versus CO

The H₂CO and CO maps (Figs. 1b and 3b) show extended spatial distributions for the observations near 1 AU. Extended sources for both species in this comet have been suggested from previous observations for heliocentric distances $R_h < 1.5$ AU (Bockelée-Morvan et al. 2000). The transitions observed here are likely to be collisionally excited. Water and CO are the primary collision partners for neutral species within the coma collision radius, $r_c \sim 10^5 \text{ km}$, of Hale-Bopp (1 AU). The CO number density within the collision radius of Hale-Bopp at 1 AU was $n(r) > 10^4 \text{ cm}^{-3}$, although it should drop off roughly as r^{-2} with distance from the nucleus r . Because of its low dipole moment (0.1 D), densities of only $(1-10) \times 10^3 \text{ cm}^{-3}$ are needed to excite the $J = 1 \rightarrow 0$ and $J = 2 \rightarrow 1$ transitions of CO. In addition, the photodestruction rate of this molecule is only $1.2 \times 10^{-6} \text{ molecules s}^{-1}$, i.e., the molecule is fairly robust against photodestruction by solar radiation. On the other hand, H₂CO has a larger dipole moment (2.3 D), and collisional excitation requires densities on the order of $\sim 10^6 \text{ cm}^{-3}$ for the $J = 1 \rightarrow 0$ and $J = 3 \rightarrow 2$ lines. Moreover, the photodissociation rate is

2.8×10^{-4} molecules s^{-1} , almost 2 orders of magnitude higher than that of CO. In addition, the production rate ratio $Q(\text{CO})/Q(\text{H}_2\text{CO})$ is ≥ 10 . For all of these reasons, CO should be far more extended than H₂CO; yet the 12 m maps indicate that these two molecules have roughly the same extent (see Figs. 1 and 3). The estimate source size scale of H₂CO is $r_s \sim 15,000$ km, similar to that of CO, $r_s \sim 19,000$ km.

As discussed, the interferometer map showed a secondary source of H₂CO, 20'' away from the comet nucleus in the tailward direction. This source may be caused by a large fragmentation event. The 12 m OTF map, observed 4 days later, also shows extended (and perhaps asymmetric) emission, although the beam size is likely contributing to this effect. The elongation, however, may be related to the second component seen in the BIMA data.

The extended distribution and differing structure of the H₂CO emission compared to CO may support independent formation mechanisms for these two species within 1 AU. Observations at 6 AU (Womack et al. 1997; Biver et al. 1997) also indicate different distributions for CO and H₂CO. Feldman et al. (2004) has suggested that the sunward-directed CO emission-line velocities of ~ 0.3 – 0.4 km s^{-1} were too high to be explained by sublimation of exposed surface CO ice, but might be explained by a phase change in water ice from amorphous to crystalline states. On the other hand, the H₂CO expansion velocity at 6 AU was nucleus centered, possibly indicative of release from icy grains (Feldman et al. 2004). Asymmetric expansions are typical of comets in which the redward versus blueward line wings do not necessarily have the same outflow velocity, such as, for example, in CH₃OH toward comet Hale-Bopp (Ikeda et al. 2002).

The data collected in the coma of P1/Halley (~ 1 AU) by the Ion Mass Spectrometer (IMS-HIS) aboard *Giotto* indicate that both CO and H₂CO arose in part from extended sources. Approximately half of the CO and most of the H₂CO were released from distributed coma sources with size scales of $\sim 10^4$ and 5000 km respectively (Eberhardt 1999; Meier et al. 1993). The IMS-HIS spectrometer showed an increasing protonated formaldehyde ion (CH₂OH⁺) concentration as the spacecraft moved away from the nucleus of comet Halley. At 1500 km from the nucleus, inside the coma contact surface, the CH₂OH⁺ abundance was calculated to be 1% of water and increased to a few percent of water at the ionopause—apparently due to an extended source (Geiss et al. 1991; ion velocity and two incidence angles affected mass/charge information; therefore, laboratory calibration was required for fitting).

4.3. An Origin in POM?

Since the first radio detection of H₂CO toward comet Halley, it has been proposed that this molecule arises generally from a source 10^3 – 10^4 km from the nucleus (Snyder et al. 1989). Missions to comet Halley also detected an extended production region of H₂CO and CO up to a few times 10^4 km from the nucleus (Festou 1999). The extended source of H₂CO was predicted to have a scale length of approximately 1.2 times the photodissociative scale length of H₂CO at 1 AU (~ 5000 km) for comet Halley, roughly 10^4 km from the nucleus (Meier et al. 1993).

The origin of the extended source of H₂CO in comets has been in debate since the Halley era. The first proposed parent of H₂CO was a polymer called polyoxymethylene or “POM” (Wickramasinghe 1975). The evidence for POMs was suggested in the 1986 *Giotto* mission encounter with comet Halley, which carried five sensor instruments used to analyze volatile material in the coma. Three of these instruments were “magnetic mass spectrometers,” NMS (neutral mass spectrometer), IMS-HERS (ion mass spectrometer–high energy range spectrometer), and IMS-HIS (IMS–high intensity mass spectrometer), and two were

energy analyzers, RPA-PICCA (Reme plasma analyzer–positive ion cluster composition analyzer) and the NMS energy analyzer. Together these instruments were able to measure neutral molecules of mass 12–50 amu and ion molecules and clusters of mass 12–100 amu with limited mass resolution and different integrities at distances of ~ 2000 , 10,000, and 60,000 km from the comet nucleus (Altwegg et al. 1999). In addition, the Halley *Vega* missions carried dust particle impact TOF (time of flight) mass spectrometers (PUMAs) to measure positive atomic and molecular ions released by dust particles. Forty-three “suitable” spectra were cumulatively evaluated for predominant, vibrationally cold, desorption molecular ions.

POM was invoked to explain the RPA-PICCA ion data, where an ordered series of mass groups centered at 31, 45, 61, 75, 90, and 105 amu was found (Korth et al. 1986; Mitchell et al. 1987; Huebner 1987). The mass groups could be explained by H₂CO chain-type molecules. Mitchell et al. (1992), with a more detailed analysis of 30 RPA-PICCA “molecular ion mass spectra” from *Giotto*, later noted that the spectra were admittedly different from those obtained by PUMA on board *Vega 1*. Other interpretations of the NMS data also disagreed with the POM identification (Meier et al. 1993). Mitchell et al. (1992) finally explained this ordered series of mass groups in their spectra as arising from a natural abundance of ion molecules composed of all possible combinations of C, H, O, and N (similar experimental results were found by Schutte et al. 1993).

Observations of a large number of comets now indicate that cometary dust grains consist predominantly of silicates (crystalline and amorphous) intimately mixed with a significant organic refractory component (e.g., Jessberger 1999; Hanner & Bradley 2004). CHON grains, which are plausible sources of radicals such as CN and C₂, long observed in comets (e.g., A’Hearn et al. 1986; Combi & Fink 1997), were discovered from the organic component samples by in situ experiments in comet Halley. H₂CO could also be released directly from these volatile organic-rich coma grains. POM is not a likely source of H₂CO because (1) a relatively large abundance of POM is required (1%–16% of the mass of the grains; Fray et al. 2004) and (2) the possible chemical pathways for producing the POM in interstellar and early solar system environments are not efficient (e.g., Allamandola et al. 1999). Instead, H₂CO is likely to be embedded in volatile grain matrices and released directly into the coma upon vaporization by solar heating, as suggested for C₂ by others (e.g., A’Hearn et al. 1986; Combi & Fink 1997).

4.4. Comet T7 LINEAR’s Second Velocity Component?

As discussed, a second component seems to be apparent in the H₂CO data at $v_{ss} \sim 4.5 \pm 0.8$ km s^{-1} and $v_{ss} \sim 4.0 \pm 0.7$ km s^{-1} with line temperatures of ~ 0.04 and 0.03 K for the $J_{K_a, K_c} = 3_{0,3} \rightarrow 2_{0,2}$ and $J_{K_a, K_c} = 3_{1,2} \rightarrow 2_{1,1}$ transitions, respectively. This component was apparently observed in OH as well. Howell et al. (2004) reported an OH excess from Arecibo observations in 2004 mid-April, of 10%–20% around a $+3$ km s^{-1} cometocentric velocity. Second velocity components have also been observed in HCO⁺ and HNC toward comet Hale-Bopp and are believed to be due to cometary fragmentation of submicron grains (Milam et al. 2004). Such grains were detected toward comet T7 LINEAR at 3.5 AU by Kawakita et al. (2004) and were believed to consist of water ice grains and silicate grains. These dirty ices could possibly also bear H₂CO and other volatile material that would be released as the grain material reaches a thermal degradation limit. The second velocity component, however, was not observed in the third line, detected almost 10 days later, indicating that the putative grain source had become inactive. The second component found

in HCO⁺ observations toward Hale-Bopp also disappeared 1–2 days later (Milam et al. 2004).

Fragmentation events in comets and/or other solar system bodies such as asteroids may play a key role in understanding the origins of prebiotic material (see review by Ehrenfreund et al. 2002). Molecules such as H₂O, H₂CO, and other organics known to be ubiquitous in comets could have detached from a cometary body and perhaps seeded planets or other objects that interact with planetary systems. These fragmentations occur multiple times over a comet orbit and can occur many times before the comet is completely destroyed. Enough material could have been ejected from these icy bodies and onto planetary surfaces to help initiate the formation of prebiotic material.

4.5. Comparison Among Various Comets

The H₂CO production rates are fairly consistent for the three comets included in this study, as well as for comet Halley, having typical $Q/Q(\text{H}_2\text{O})$ ratios of 0.1%–2% at ~1 AU. Even though these values were determined from an extended source model, the results are still in good agreement with others. The multiple-comet study by Biver et al. (2002) found the $Q(\text{H}_2\text{CO})/Q(\text{H}_2\text{O})$ ratio in 13 comets to be between 0.13% and 1.3%. These values were determined from a distributed source with a Haser equivalent density distribution (Biver et al. 2002). These results suggest that there is some chemical homogeneity among the comets, at least for H₂CO.

Observations of H₂CO at 4 AU indicate a higher $Q(\text{H}_2\text{CO})/Q(\text{H}_2\text{O})$ ratio of ~2% for a grain source, or 0.5% for a parent species, indicating a non-water-driven chemistry at large heliocentric distances. These results are in good agreement with the long-term chemical evolution studies of Hale-Bopp conducted by Biver et al. (2002) and Womack et al. (1997). The steep dependence of the formaldehyde production rate on R_h is also confirmed.

5. CONCLUSIONS

Observations of H₂CO toward comet Hale-Bopp demonstrate that this molecule has an extended distribution, indicating that it

originates at least in part from a source other than the comet nucleus. A likely source of H₂CO in comets may be coma grains composed of an organic-dominated silicate-organic matrix. These grains are released from the nucleus and are vaporized or thermally degraded by solar heating, ejecting organic molecules into the expanding coma. Hence, organic molecules with short photodissociation lifetimes (<10⁴ km) such as H₂CO can be found much farther from the comet nucleus than their photodestruction rates would suggest. A grain source for H₂CO may also explain structure observed in the BIMA maps of this molecule, as well as secondary velocity components observed in other comets such as comet T7 LINEAR. Fragmentation of comet dust in the coma, as well as material rich in carbon (e.g., C₂ and C₃) released from jets (A'Hearn et al. 1986), may contribute significantly to the carbon that is thought to have been deposited in the Earth's atmosphere over the centuries, as suggested by Ehrenfreund et al. (2002). Results also confirm that H₂CO cannot be a significant source of CO in Hale-Bopp, since the production rates differ by a factor of ≥10.

We thank D. K. Yeomans for ephemerides assistance and G. Engargiola, T. Helfer, W. Hoffman, R. L. Plambeck, and M. W. Pound for invaluable technical contributions. This material is based on work supported by the National Aeronautics and Space Administration through the NASA Astrobiology Institute under Cooperative Agreement CAN-02-OSS-02 issued through the Office of Space Science. S. N. M. would like to thank the Phoenix Chapter of ARCS, specifically Mrs. Scott L. Libby, Jr. endowment, for partial funding. This work was partially funded by NASA NAG5-4292, NAG5-4080, NAG5-8708, and NGT5-0083; NSF AST 96-13998, AST96-13999, AST96-13716, AST96-15608, and AST99-81363; and the Universities of Illinois, Maryland, and California, Berkeley. M. W. was funded by NSF AST 9625360, AST 9796263, and AST 0098583 and NASA NAG5-4349. L. A. was partially supported by NSF 0216226.

REFERENCES

- A'Hearn, M. F., Hoban, S., Birch, P. V., Bowers, C., Martin, R., & Klinglesmith, D. A. 1986, *Nature*, 324, 649
- Allamandola, L. J., Bernstein, M. P., Sandford, S. A., & Walker, R. L. 1999, *Space Sci. Rev.*, 90, 219
- Altwegg, K., Balsiger, H., & Geiss, J. 1999, *Space Sci. Rev.*, 90, 3
- Biver, N., et al. 1997, *Science*, 275, 1915
- . 2002, *Earth Moon Planets*, 90, 5
- Bockelée-Morvan, D., et al. 2000, *A&A*, 353, 1101
- Combi, M. R., & Fink, U. 1997, *ApJ*, 484, 879
- Combi, M. R., & Smyth, W. H. 1988, *ApJ*, 327, 1026
- Crovisier, J., et al. 2004, *A&A*, 418, 1141
- Eberhardt, P. 1999, *Space Sci. Rev.*, 90, 45
- Ehrenfreund, P., et al. 2002, *Rep. Prog. Phys.*, 65, 1427
- Feldman, P. D., Cochran, A. L., & Combi, M. R. 2004, in *Comets II*, ed. M. C. Festou, H. U. Keller, & H. A. Weaver (Tucson: Univ. Arizona Press), 425
- Festou, M. C. 1999, *Space Sci. Rev.*, 90, 53
- Fray, N., Benilan, Y., Cottin, H., & Gazeau, M.-C. 2004, *J. Geophys. Res. Planets*, 109, E07S12
- Friedel, D. N., et al. 2005, *ApJ*, 630, 623
- Geiss, J., et al. 1991, *A&A*, 247, 226
- Gombosi, T. I., & Horanyi, M. 1986, *ApJ*, 311, 491
- Halfen, D. T., et al. 2006, *ApJ*, 639, 237
- Hanner, M. S., & Bradley, J. P. 2004, in *Comets II*, ed. M. C. Festou, H. U. Keller, & H. A. Weaver (Tucson: Univ. Arizona Press), 555
- Harris, W. M., Scherb, F., Mierkiewicz, E., Oliverson, R., & Morgenthaler, J. 2002, *ApJ*, 578, 996
- Hollis, J. M., Jewell, P. R., Lovas, F. J., & Remijan, A. 2004, *ApJ*, 613, L45
- Hollis, J. M., Vogel, S. N., Snyder, L. E., Jewell, P. R., & Lovas, F. J. 2001, *ApJ*, 554, L81
- Howell, E. S., Lovell, A. J., & Schloerb, F. P. 2004, *IAU Circ.*, 8329, 2
- Huebner, W. F. 1987, *Science*, 237, 628
- Huebner, W. F., Keady, J. J., & Lyon, S. P. 1992, *Ap&SS*, 195, 1
- Ikeda, M., Kawaguchi, K., Takakuwa, S., Sakamoto, A., Sunada, K., & Fuse, T. 2002, *A&A*, 390, 363
- Jessberger, E. K. 1999, *Space Sci. Rev.*, 90, 91
- Kawakita, H., et al. 2004, *ApJ*, 601, L191
- Kolokolova, L., Hanner, M. S., Lvasseur-Regourd, A.-Ch., & Gustafson, B. Å. S. 2004, in *Comets II*, ed. M. C. Festou, H. U. Keller, & H. A. Weaver (Tucson: Univ. Arizona Press), 577
- Korth, A., et al. 1986, *Nature*, 321, 335
- Küppers, M., Hartogh, P., & Villanueva, G. 2004, *AAS Planet. Sci. Meet. Abs.*, 36, 25.05
- Lamy, P. L., & Perrin, J. M. 1988, *Icarus*, 76, 100
- Lecacheux, A., Biver, N., Crovisier, J., & Bockelée-Morvan, D. 2004, *IAU Circ.*, 8304, 2
- Lis, D. C., et al. 1999, *Earth Moon Planets*, 78, 13
- Magee-Sauer, K., Dello Russo, N., DiSanti, M. A., Bonev, B., Gibb, E. L., & Mumma, M. J. 2004, *AAS Planet. Sci. Meet. Abs.*, 36, 25.03
- Meier, R., Eberhardt, P., Krankowsky, D., & Hodges, R. R. 1993, *A&A*, 277, 677
- Milam, S. N., Savage, C., Ziurys, L. M., & Wyckoff, S. 2004, *ApJ*, 615, 1054
- Mitchell, D., Lin, R., Carlson, C., Korth, A., Reme, H., & Mendis, D. 1992, *Icarus*, 98, 125
- Mitchell, D., et al. 1987, *Science*, 237, 626
- Mumma, M. J., Weaver, H. A., Larson, H. P., Davis, D. S., & Williams, M. 1986, *Science*, 232, 1523
- Remijan, A., et al. 2006, *ApJ*, 643, 567
- Sault, R. J., Teuben, P. J., & Wright, M. C. H. 1995, in *ASP Conf. Ser. 77, Astronomical Data Analysis Software and Systems IV*, ed. R. A. Shaw, H. E. Payne, & J. J. E. Hayes (San Francisco: ASP), 433

- Schutte, W. A., Allamandola, L. J., & Sandford, S. A. 1993, *Icarus*, 104, 118
- Shoolery, J. N., & Sharbaugh, A. H. 1951, *Phys. Rev.*, 82, 95
- Snyder, L. E., Palmer, P., & de Pater, I. 1989, *AJ*, 97, 246
- Sorrell, W. H. 2001, *ApJ*, 555, L129
- Wickramasinghe, N. C. 1975, *MNRAS*, 170, 11P
- Womack, M., Festou, M. C., & Stern, S. A. 1997, *AJ*, 114, 2789
- Womack, M., Pinnick, D. A., Mangum, J. G., Festou, M. C., & Stern, S. A. 2000, in *ASP Conf. Ser. 217, Imaging at Radio through Submillimeter Wavelengths*, ed. J. G. Mangum & S. J. E. Radford (San Francisco: ASP), 82
- Woodney, L. M., et al. 1996, *IAU Circ.*, 6408, 2